Journal of Constructional Steel Research 154 (2019) 250–262

Contents lists available at ScienceDirect

Journal of Constructional Steel Research

Innovative steel 3D trusses for preservating archaeological sites: Design and preliminary results

Gianmaria Di Lorenzo, Enrico Babilio, Antonio Formisano *, Raffaele Landolfo

Department of Structures for Engineering and Architecture (DiSt), University of Naples "Federico II", Naples, Italy

ARTICLE INFO

Article history:
Received 19 March 2018
Received in revised form 9 December 2018
Accepted 10 December 2018
Available online 20 December 2018

Keywords:
Steel 3D lattice beams
Structural glass slab
Cultural assets
Archaeological sites
Capacity design criteria
Simplified design methods

ABSTRACT

Steel three-dimensional lattice trusses are highly efficient technical solutions to cover large spans, especially when single members are not provided with intermediate restraints able to prevent lateral-torsional buckling phenomena. In the present paper, a compound structure made of steel lattice beams and structural glass slabs is proposed for protection of monumental and archaeological sites. Due to both the risk exposure of monumental heritage to be protected and the use of structural glass, the definition of an appropriate design criterion is mandatory in order to avoid brittle collapse mechanisms. The attention is herein paid to the design procedure, with a brief description of basic ideas behind and the main focus on the parametric capacity design of the structure. The proposed procedure, whose validity is quite general, has been herein implemented by linear numerical analyses, which represent the basic step for further refined analysis aimed at erecting a full-scale prototype to be experimentally tested.

© 2018 Elsevier Ltd. All rights reserved.

1. Introduction

The preservation of cultural heritage may be assured by adopting rules of indirect protection aimed at avoiding damages to both immovable objects and the surrounding landscape and environment [1,2]. In case of archaeological sites and artefacts, the protection, and possible musealization following the digging up phase, is usually made by using covering structures, which should be light, able to both cover large spans without intermediate supports and ensure accessibility to assets and easy to be assembled, maintained, disassembled and even possibly reused in other sites [3]. Fulfilling, in a satisfactory manner, such list of requirements, glued laminated timber structures can be used for coverings sites and assets to be protected, since they well-combine the typical colouring and appearance of timber with a slight cracking pattern, distinctive of a time-stamped ruin [4,5]. In terms of material, a competitor and a good alternative to the glued laminated timber is provided by the weathering steel, which similarly can be integrated into the context, thanks to its typical brownish colouring, providing at the same time a high durability. The present paper is aimed at proposing a new three-dimensional (3D) truss made of weathering steel designed as primary structure for supporting floors made of structural glass slabs, without needs for secondary members. The innovative steel beam, mainly designed for archaeological sites [6], is thought to be patented, after a properly developed assessment phase, as a prefabricated industrial product. 3D trusses or lattice beams are members with longitudinal dimensions prevailing on transverse ones. They belong to the largest family of 3D structures [7], which are typically characterised by both a three-dimensional behaviour (space behaviour) and an axial stress regimen (lattice behaviour). Composed of tetrahedral and hemi-octahedral repetitive modules made of metal members, generally with pipe sections mutually connected to each other by either welding or bolted connections, these systems allow increasing the structural performance by spacing out the chords, as in case of plane (2D) lattice beams. However, with respect to the 2D beam solution, high torsional and out-of-plane flexural rigidities make the 3D solution more convenient, mainly in the cases where self-weight support during construction is required or lateral restraints against lateral-torsional buckling are absent [8]. For the 3D lattice beam under investigation, due to the high exposure of assets to be protected, often located in medium-high seismic areas, and the presence of structural glass panels [9,10], a suitable project methodology matching capacity design and fail-safe principles is proposed in order to design members with ductile and robust behaviour under static or dynamic vertical actions. The current work illustrates preliminary the beam analysis and design, while the assessment phase, currently in progress, will be only briefly shown for the sake of completeness, considering that the whole numerical and experimental characterization of the investigated beam will be treated in a future work.

The paper is organized as follows. Firstly, a brief historical review and state of art on the typology of steel 3D lattice beams is given (Section2). Subsequently, the structural conception guiding the design

* Corresponding author.
E-mail addresses: gianmaria.dilorenzo@unina.it (G. Di Lorenzo), enrico.babilio@unina.it (E. Babilio), antoform@unina.it (A. Formisano), landolfo@unina.it (R. Landolfo).

https://doi.org/10.1016/j.jcsr.2018.12.006
0143-974X/© 2018 Elsevier Ltd. All rights reserved.

List of symbols

a, a_{opt}	Length and optimal length of tie (batten) plates along top chord
A, A_0, A_n	Generic, gross, net cross-sectional areas
$A_{v,z}$, A_w	Effective shear area and web net area
B	Width of the lattice beam cross-section
B_x, B'	Measures of the bases of the hemi-octahedral module eccentricity
e	Design stress
E_d	Design load per unit length
F_{Ed}	Design load per unit length producing the yielding of the bottom chord
$F_{pl,Rd}$	Yield stress
$f_{(y,k)}$	Lattice beam weight per unit length
G_k	Dead load and variable actions per unit area
g_k, q_k	Height of the lattice beam cross-section
H	Theoretical height of both the hemi-octahedral module and the lattice beam
H'	Cross-section gyration radius
i	Inter-spacing between two lattice beams
i_T	Second moment of area along strong (y) and weak (z) axes
I_y, I_z	Torsional (t) and warping (w) constants
I_t, I_w	L_{min}, L_{max} Net length, total length, minimum length and maximum length of the lattice beam
L, L',	Theoretical length of the inclined sides of the hemi-octahedron
l'	Design global bending moment (due to F_{Ed})
$M_{Ed,glob}$	Maximum (demand) axial force in bottom chord
$N_{Ed,c}$	Maximum (demand) axial force in diagonal web members
$N_{Ed,d}$	Maximum axial force on diagonal rods of a plane Warren isostatic truss
N_{max}	Axial load producing the yielding in the mid-section of the bottom chord
$N_{pl,Rd}$	Number of hemi-octahedral modules in a lattice beam
n_x	Cross-sectional shape and global shape ratios
r_{BH}, r_{HL}	Generic property of a section and a benchmark profile (for efficiency ratio)
S,S_{SQ}	Thickness of basic profile for the top chord
t	Thickness of plates used for stiffening bottom chord nodes
t_f	Design global shear force (due to $F_{pl,Rd}$)
$V_{Ed,glob}$	Width of tie plates (also distance between holes) along top chord
w	Elastic section modulus
$W_{el,y}$	Axes of the Cartesian reference frame
x,y,z	Extra-length of the lattice beam, double of the support length
Δ	Normalized slenderness
$\overline{\lambda}_{f,z}$	Efficiency ratio
ρ_s	Over-strength coefficient and additional over-strength coefficient for top chord members
Ω, Ω_0	

List of abbreviations and acronyms

2D, 3D	Two-dimensional, Three-dimensional
BB.CC.	*Beni Culturali* (Cultural Heritage), name of the proposed lattice beam
C-RHS	Cellular rectangular hollow section (referred to BB.CC. beams)
C, R, SQ	Channel, round, square profiles (standard profiles)
CHS,	RHS, SHS Circular, rectangular, square hollow sections (standard profiles)
CF, HR	Cold formed, hot rolled (with reference to standard profile)
FEM	Finite Element Method
SLS, ULS	Serviceability Limit State, Ultimate Limit State

of the compound structure made of lattice beams and glass slab is provided (Section3). Afterwards, a detailed focus on the design criteria implemented for the beam and the related results are illustrated (Sections 4–6). Finally, even if beyond the scope of this work, a preliminary overview on the overall activities devoted to the performance assessment of the beam are given (Section7), whereas the study conclusions are drawn in the last paragraph (Section8).

2. A brief historical review and state of art on steel 3D beams

The early studies on the structural behaviour of space systems date back to the end of the eighteenth century thanks to August Föppl, who defined the equation for investigating the three-dimensional kinematic behaviour of systems made of rods in his dissertation “Das Fachwerk Im Raum” (*The space lattice girder*) [11]. On the other hand, the first applications of pre-fabricated 3D lattice structures, due to Alexander Graham Bell, were made during the early 1900s. Bell immediately understood the potential of such a constructive system and, as a consequence, experimented the use of tetrahedral and octahedral modules, obtained by assembling metal bars and joints, to produce gliders and wing structures. However, several decades passed to see developed technologies able to produce, on an industrial scale, connections combining reliable performance with ease of erection [12]. Among many others, it is worth mentioning the so-called Mero system, developed in Germany since 1943 by Max Mengeringhausen, which is a constructive system still used worldwide for building double-layer truss grids. However, only after the Second World War many patents were developed aiming at encouraging the use of industrialised systems in the field of steel structures [13].

A fundamental contribution to the spread of space lattice structures, mainly as geodesic domes, was due to Walther Bauersfeld, a Berliner physicist and engineer, who developed the first structural solution in 1926 and further, since the 1950s, to Richard Buckminster Fuller.

The 1970s represented the “golden age” of prefabricated 3D lattice structures, that nowadays are finding a new impetus for the construction of complex geometries made of steels or aluminium alloys [14], used either in the civil field for the construction of large roofing and towers [15] or in the industrial one for automotive, lifting and offshore applications.

Currently, a further impulse to the development of this structural typology is coming from the widespread use of pipe and box profiles in any engineering field through the CAD-CAM technology (and nowadays also by the Building Information Modelling in the civil engineering sector), thanks to the improvement of the metal cutting and welding techniques allowing for designing and producing very complex structural nodes [16]. Furthermore, the development of robust multi-objective optimization algorithms and parametric design tools, often embedded also in commercial structural analysis software packages, is contributing to the diffusion of metal space structures.

3. The constructive system

3.1. Premise

The constructive system adopted for a covering composite structure made of primary steel 3D lattice beams and glass slab (see Fig. 1, to which we refer for notations), specifically designed for safeguarding and exploiting archaeological and cultural heritage sites, is herein

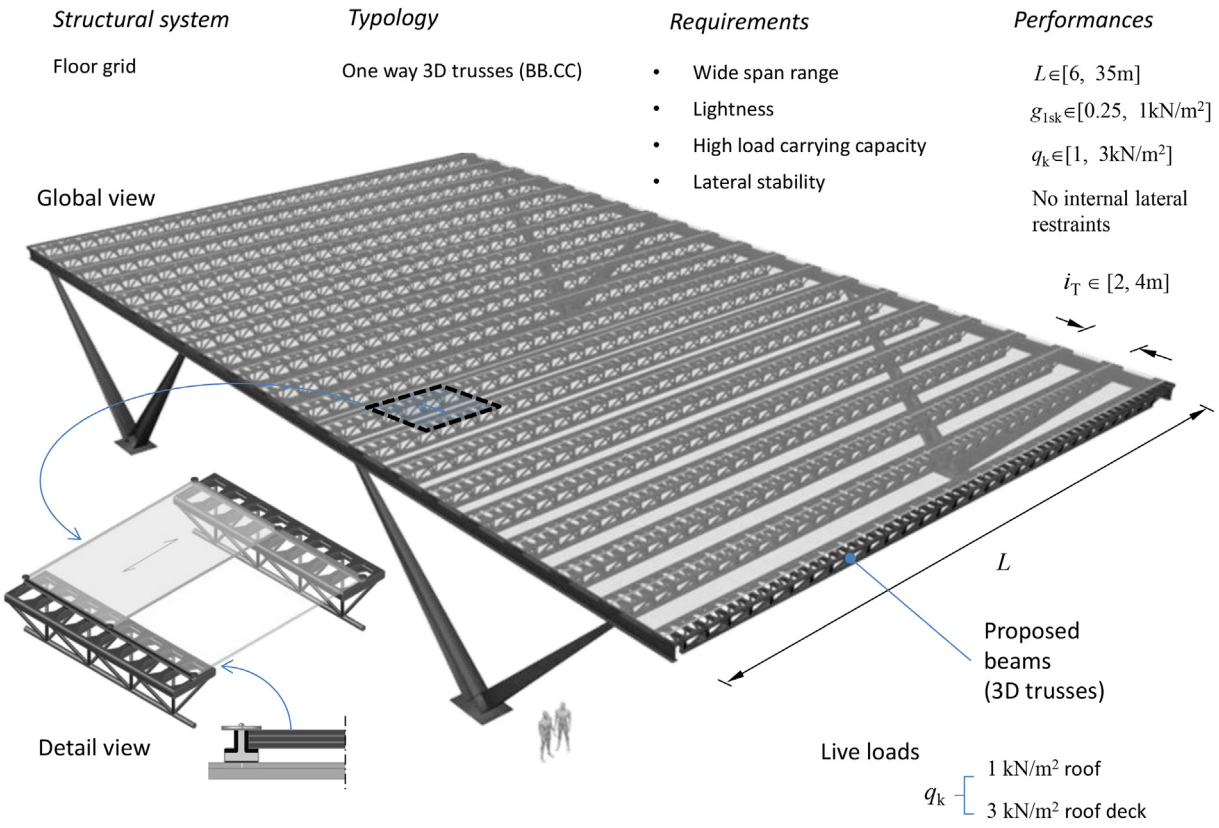

Fig. 1. The pictorial view of the proposed roof structure.

described. In order to accomplish the design tasks, a properly tailored methodology is setup.

The lattice beams, hereinafter referred to as BB.CC. (Italian acronym of *Beni Culturali*, which is translated in English as Cultural Heritage), are made of S355J2W steel, also designated with the numerical code 1.8965. The use of such a special steel is required according to three reasons: a) mechanical, due to its strength and toughness; b) durability against atmospheric precipitations and air pollution, thanks to its enhanced corrosion resistance; c) aesthetic, since its typical brownish colour makes it very suitable for applications into ancient structures. As seen in Fig. 1, BB.CC. beams are placed parallel to each other at a given distance, without intermediate supports, to form the primary structure of the coverage, which is made of structural laminated glass panels surmounting the beams through specifically designed guides. Among other possibilities, it should be noticed that glass panels, if appropriately designed and coated, allow for the proper illumination of assets, contemporary assuring their protection from effects of solar radiation [17].

3.2. Details on steel lattice BB.CC. Beams

In this section the focus is mainly devoted to BB.CC. beams, which are obtained by welding to each other European standard profiles. As a frame of reference it is assumed a Cartesian triad having the axes *x*, *y* and *z* along the length (*L*), the cross-section width (*B*) and the height (*H*) of the beam, respectively. From a geometric point of view, the architecture of any BB.CC. beam is composed as a sequence of downward hemi-octahedrons (with sides B_x and B' and height H') with interposed tetrahedrons (see Fig. 1 and Fig. 4, the latter used for geometric relations between *H* and H' and between *B* and B'). Structurally we can distinguish top and bottom chords mutually connected by web members.

Starting from an initial cold-formed Rectangular Hollow Section (RHS), produced according to the EN 10219-1 [18] and EN 10219-2 [19] standards, the top chord member is built as a castellated beam as follows (see Fig. 2). The RHS profile is longitudinally cut in two hemi-profiles subsequently assembled through welded tie plates, which allow for suitably distancing the hemi-profiles, reducing geometric tolerances during the assembly as required by the EN 1090-2 code [20]. These plates have also the task to stiffen locally the top chord-web member nodes and even to support the glass slab guides, which are put in the middle of tie plates for eliminating torsional effects induced by the floor on the beam. The relevant design parameters for the top-chord are, indeed, length *a* and the width *w* of the tie plate, optimised the former to reduce machining and material waste, the latter to confer lateral stability to the lattice beam. When finished, the top-chord profile have octagonal holes (see Fig. 2), whose idea has been fundamentally inspired by cellular beams with hexagonal holes manufactured from standard IPE 200, 300 and 400 profiles by the ArcelorMittal company. It is worth of noting that, although obtained from standard profiles, the new member contains a relevant innovation, since its manufacturing process allows for introducing a new product category, herein called as Cellular Rectangular Hollow Section (C-RHS). Such a category enlarges, in fact, the range of commercial European RHS profiles, whose cross-section height currently reaches at most 400 mm in the cold-formed (CF) profiles and 500 mm in the hot-rolled (HR) ones.

The bottom chord is made of hot-rolled round (R) or square (SQ) profiles, or even, in case of very long trusses, of Square Hollow Section (SHS) members. The bottom chord nodes are designed as fully rigid joints and they are stiffened with plates having thickness (t_f) close to that of top chord members. Finally, web members are made of R bars or Circular Hollow Section (CHS) profiles.

3.3. Nomenclature and products

With the aim to consider prefabricated beams able to cover spans from 6 to even >30 m, three values of *H*, corresponding to three product families (Fig. 3), conventionally named as "short" ($H = 600$ mm), "medium" ($H = 900$ mm) and "high" ($H = 1200$ mm) beams, are considered. Within the same product family, a beam is selected through the thickness *t* of the basic RHS profile used for the top chord. Consequently,

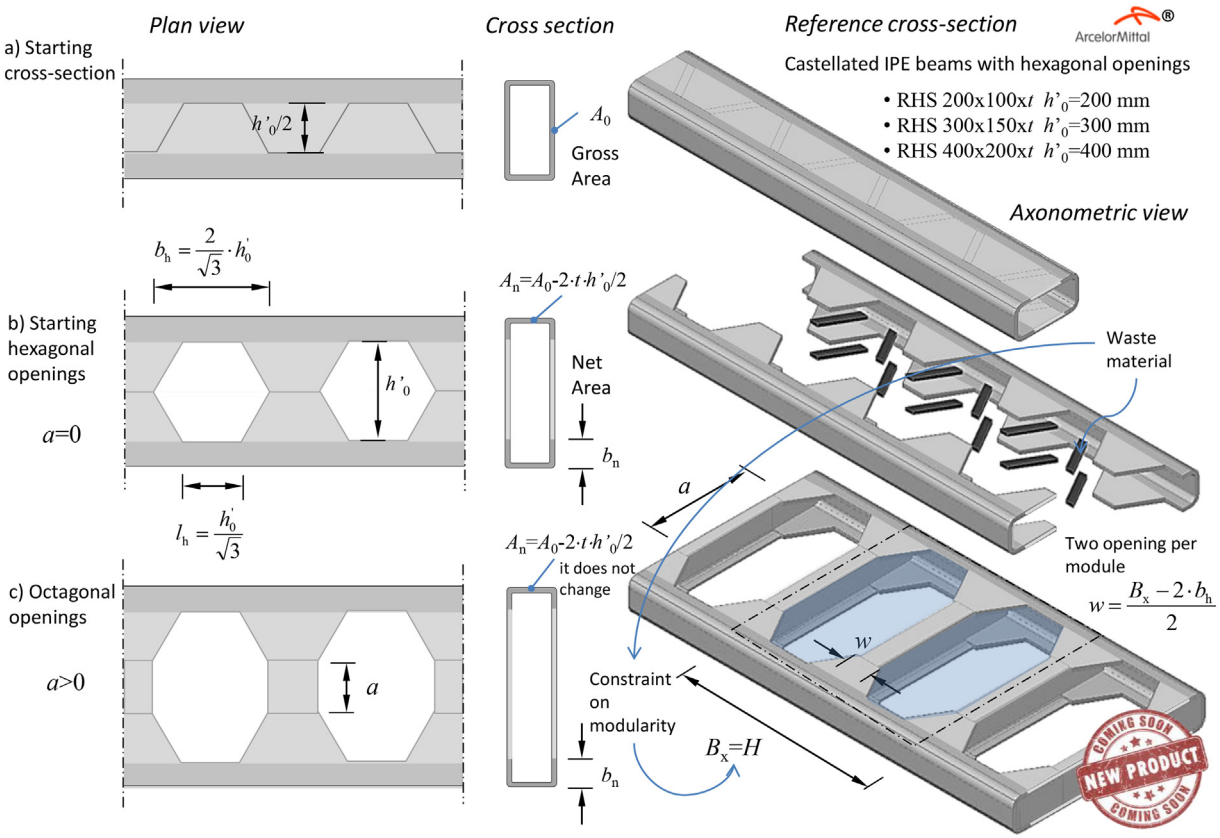

Fig. 2. Net cross-section area and manufacturing process of a Cellular Rectangular Hollow Section (C-RHS) profile.

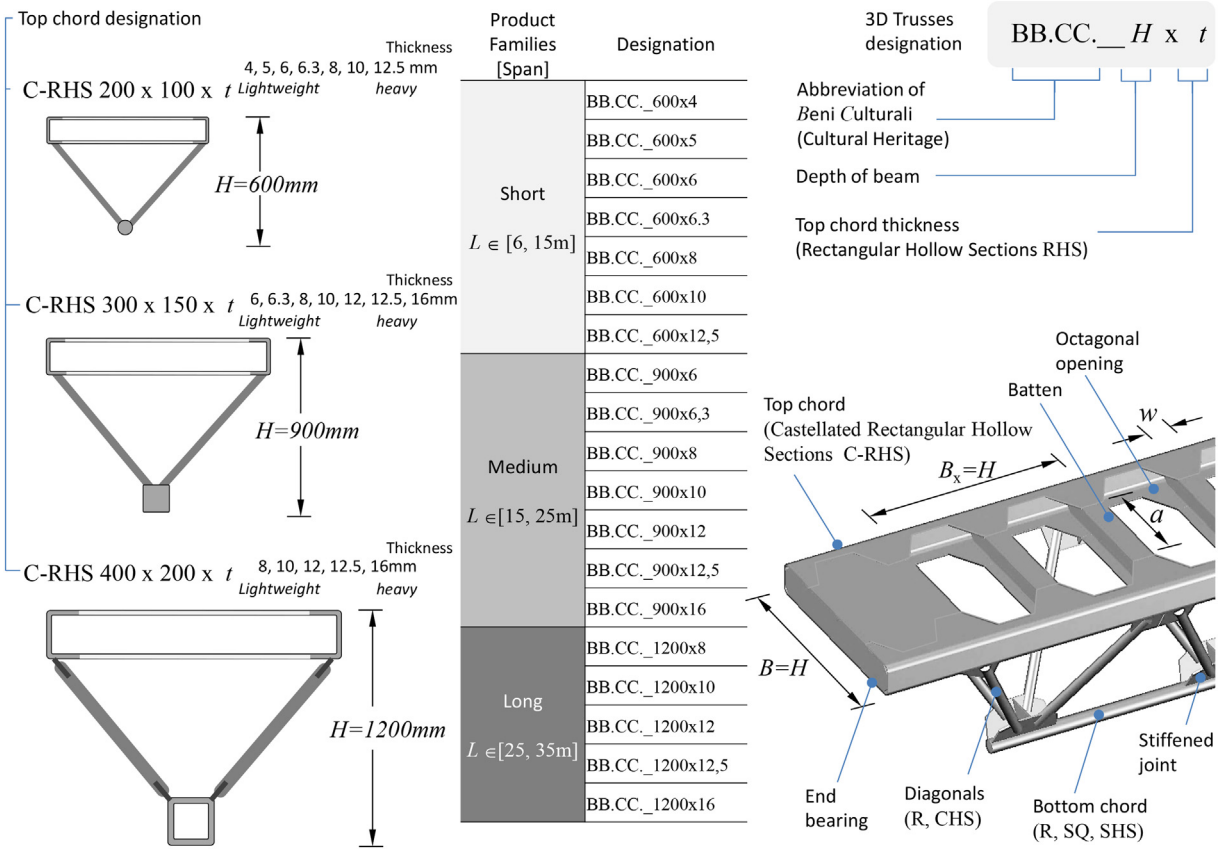

Fig. 3. BB.CC. beams: designation and families of products.

the generic beam is uniquely identified by the acronym "BB.CC. $H \times t$". Hence, as for HE beams, also BB.CC. beams can be referred to as light, middle and heavy profiles, depending on the chosen thickness t (see Fig. 3). Alongside with the process and product innovations discussed before, another advantage of using the C-RHS profile instead of the solution using two hollow profiles is that there is no need to use diagonals to stabilise the top chord in its plane.

BB.CC. beams have different performance requirements depending on the span (L), the dead loads (g_k), the variable actions (q_k) and the spacing among members (i_T).

It is noteworthy that these beams are essentially thought and designed as serial products that, due to their morphological and geometric features, comply with the character of modular constructions, as prescribed by the ISO1006 standard [21], which adopts the basic module $M = 300$ mm to favour the building industrialization process.

Indeed, the main dimensions of BB.CC. beams, namely L, B and H, are multiples of M. It is found that, for any given H, the best value of the width B, as well as of the hemi-octahedron side B_x, is selected so that $B{=}B_x = H$ (see Figs. 2 and 3). Moreover, the number of hemi-octahedronsn_x and the length L are connected to each other by the relationship $L = n_x B_x$. Thus, we may conclude that the only exception to the modularity rule is given by an extra-length ($\Delta/2$), which takes into account the size of the end bearing device. Thus, the total length to be considered in the design phase is given by $L' = L + \Delta$.

4. Design criteria

4.1. Foreword

As stated before, the high exposure of cultural assets to be protected, often placed in medium-high seismicity areas, and the use of structural glass as roofing system require the definition of an adequate design methodology based on the capacity control criterion to avoid early brittle collapse mechanisms and, therefore, to favour ductile failures of beams under vertical actions. In particular, the most preferable ductile mechanisms are given by the failure under tensile actions of the bottom chord. On the other hand, the brittle mechanisms that should be limited are, for example, either the instability of end diagonal members (global shear collapse) or the buckling of compressed chord, which can trigger lateral-torsional buckling of the whole beam in absence of torsional restraints, compromising the integrity of the upper structural glass slab. Other brittle mechanisms may be induced by the failure of both joints and end supports, the latter being prevented by the extension (due to the extra-length $\Delta/2$) and possible stiffening of the top chord.

4.2. The proposed methodology

Depending on the beam span (L) and weight (G_k), the dead loads (g_k), the variable actions (q_k), the spacing among members (i_T), according to the Schwedeler's approach [22], the maximum demand axial load in the bottom chord ($N_{Ed,c}$) is given by:

$$N_{Ed,c} = \frac{M_{Ed,glob}}{H'} = \frac{F_{Ed}\, L'^2}{8\, H'} \tag{1}$$

being $F_{Ed} = (1.3\, g_k + 1.5\, q_k)\, i_T + 1.3\, G_k$ a uniformly distributed vertical load applied to a simply supported beam of length L' and height H' (lattice beam total length and theoretical height, this latter as seen in Fig. 4). Evaluated the demand in terms of axial, the bottom chord profile (R, SQ or SHS) is selected in function of the considered beam family.

Then, the design of the top chord follows. The demand axial load is amplified by adopting a suitable over-strength coefficient Ω to both

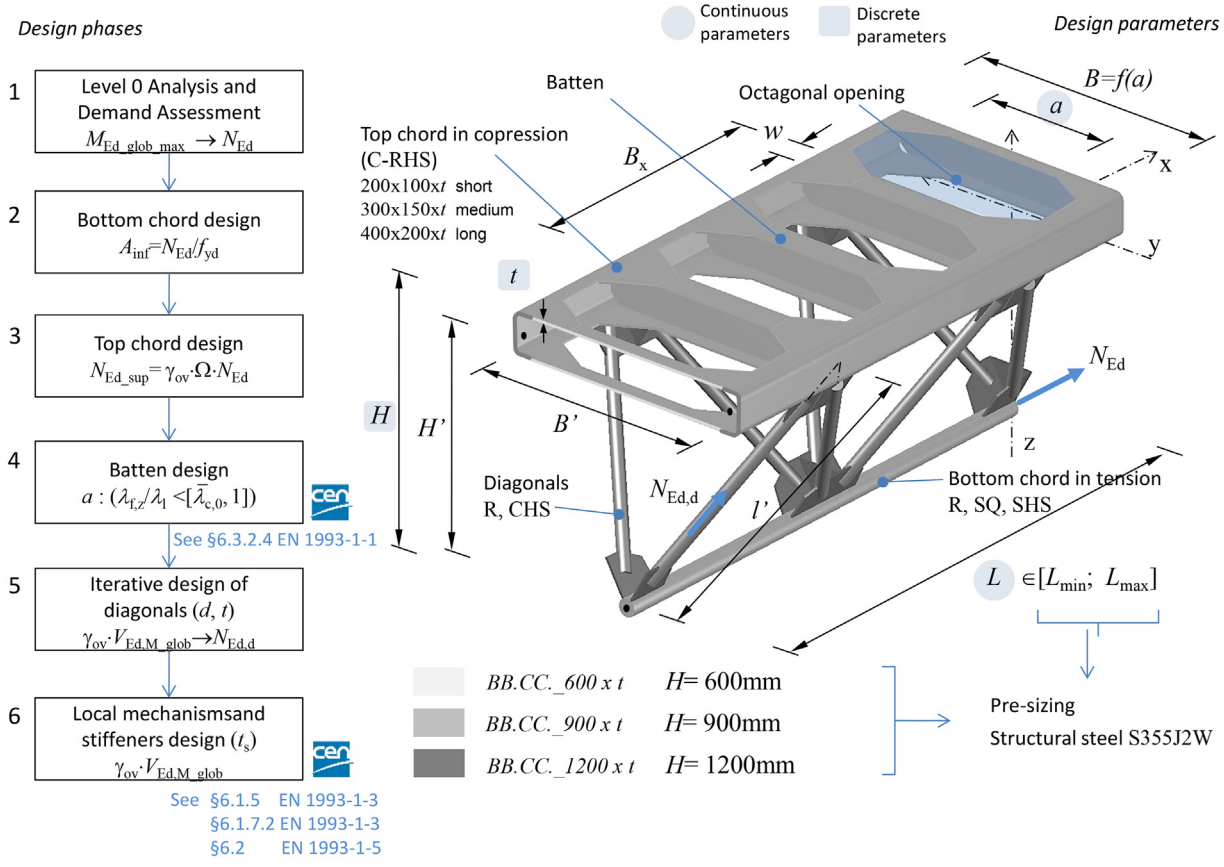

Fig. 4. Capacity control design methodology for space lattice trusses.

favour the taut bottom chord yields before the compressed top one and compensate for any performance decrease that may arise in this latter. The expression to obtain Ω is provided as follows:

$$\Omega = \frac{N_{pl,Rd}}{N_{Ed,c}} + \Omega_0 \tag{2}$$

where $N_{pl,\,Rd}$ is the yielding axial load in the mid-section of the bottom chord and Ω_0 is an additional over-strength factor. In the design phase, referring to the gross area A_0 (Fig. 2) of the basic RHS profile, the additional over-strength coefficient takes into account the decrease in capacity associated with the section reduction (net area A_n) due to the profile cutting and offsetting, as well as to the possible local or global (lateral-torsional) buckling phenomena not properly evaluated during the sizing of members.

The lateral-torsional buckling of the truss, associated to the instability of the compressed chord, is instead controlled by searching for the optimal value of the parameter *a*, that defines the batten plate size and, then, of the beam width *B*.

By adopting the simplified assessment method provided in [23], also reported in the § 6.3.2.4 of the Eurocode 3–Part 1.1 [24], the beam lateral buckling is avoided by limiting the normalized slenderness of the top chord net section $\overline{\lambda}_{f,z}$, evaluated with reference to the *z*-axis, in the range between the threshold value $\overline{\lambda}_{c,0}$ and 1. Such a simplified methodology, which is generally valid, is suitable for symmetric cross-sections, as those under investigation. Subsequently, by imposing the plastic failure of the bottom chord (plastic hinge in the mid-section), both the limit load $F_{pl,\,Rd}$ and the associated global shear $V_{Ed,\,glob}$ are determined. These actions are used to iteratively design the compressed diagonals for different values of the beam span, within a plausible range of lengths $[L_{min};\, L_{max}]$ of each BB.CC. beam family. The design axial force $N_{Ed,\,d}$ along the diagonal members is attained near the lattice supports and is estimated as.

$$N_{Ed,d} = N_{max}\frac{l'}{\sqrt{B_x^{\,2} + 4H'^2}} = \pm\frac{(n_x - 1)\,F_{pl,Rd}\,B_x}{8H'}\sqrt{B_x^{\,2} + B'^2 + 4H'^2} \tag{3}$$

where the (theoretical) length l' of the inclined sides of the hemi-octahedron is computed as.

$$l' = \frac{1}{2}\sqrt{B_x^{\,2} + B'^2 + 4H'^2} \tag{4}$$

B_x, B' and H' being the already defined module's measures (see Fig. 4 for reference) and.

$$N_{max} = \pm(n_x - 1)\frac{F_{pl,Rd}\,B_x}{4H'}\sqrt{B_x^{\,2} + 4H'^2} \tag{5}$$

is the maximum axial force on diagonal rods of the 2D Warren isostatic truss obtained by projecting the 3D beam onto its longitudinal mid-plane (i.e. the *x*,*z*-plane).

The procedure ends by checking that no local mechanism appears in the end bearings due to shear and crippling crisis of the top chord web. To this purpose, in such areas the member is transversely stiffened by plates having adequate thickness.

The capacity models used for local checks towards shear and crushing of channel (C) profiles are given in § 6.1.5 and in § 6.1.7.2 of the EN 1993-1-3 code [25], respectively. Whenever necessary, evaluation of the transverse stiffening can be performed according to the models reported in § 6.2 of the EN 1993-1-5 code [26], with the effective section defined in § 9.1 of the same standard.

In order to ensure the activation of the ductile collapse mechanism produced by the yielding of the bottom chord, the sizing of compressed chord, end-diagonals and bearings without premature collapse should be performed considering the uncertainties of the effective yield stress value. This is achieved by multiplying the design stresses E_d for the material over-strength coefficient γ_{ov}, given by the current national and European regulations as equal to 1.10 for S355 grade steels. Such a coefficient should be evaluated by taking into account the uncertainties related to the different steel type, to the currently available production processes [27] and to the thickness of adopted steel products. However, it is noticed that the entire procedure takes into account full-strength joints among members. Thickness of gusset plates and their effective width are related to dimensions of web bracing members according to the Whitmore's method [28,29], which considers a stress diffusion

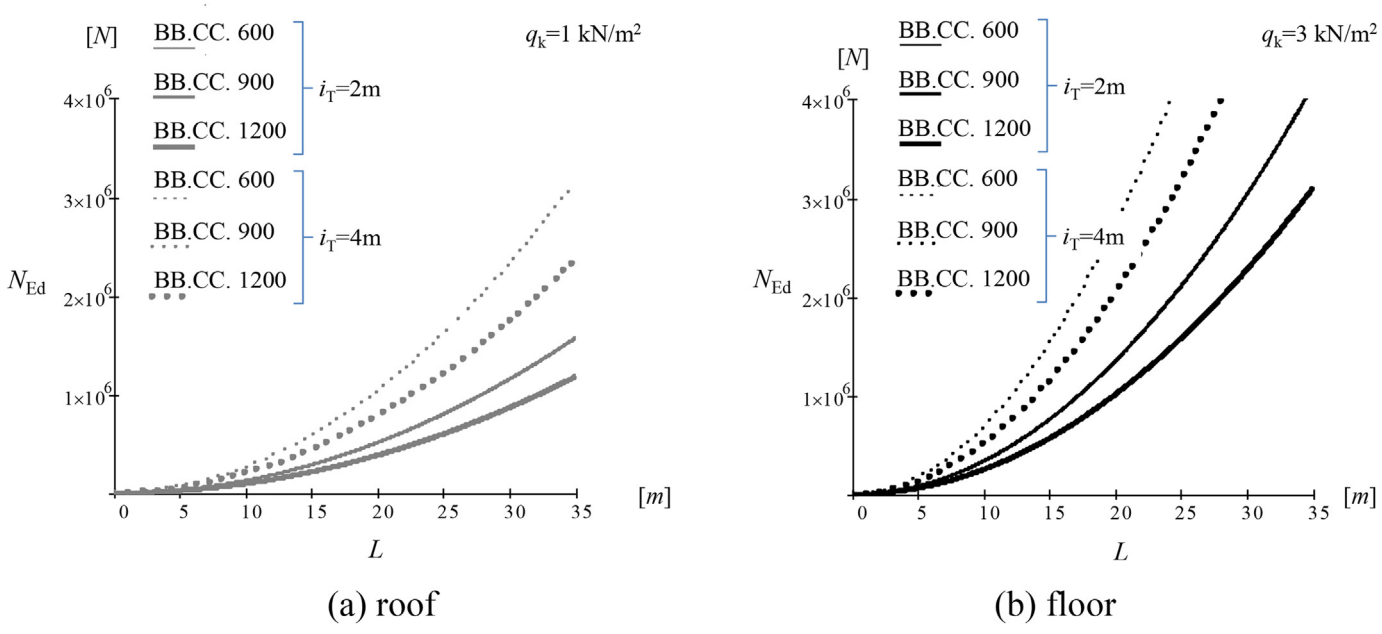

Fig. 5. Axial force $N_{Ed,c}$ (demand) in the bottom chord as a function of beam length and spacing.

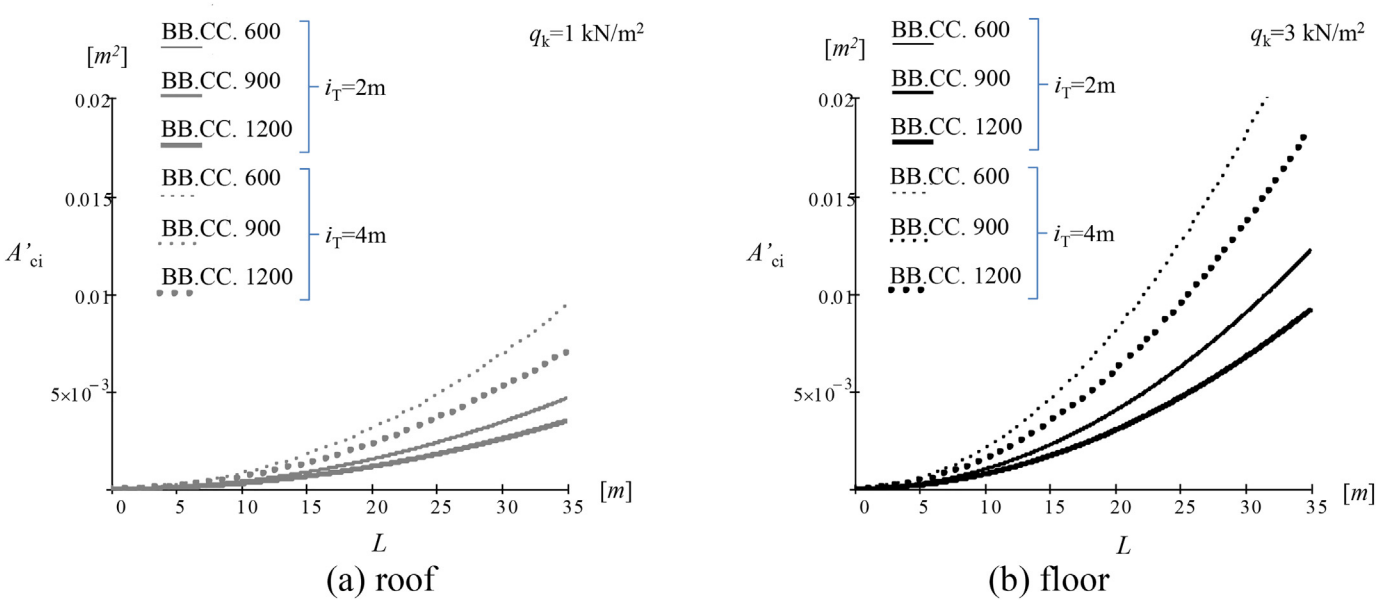

Fig. 6. Theoretical cross-sectional area of the bottom chord as a function of beam length and spacing.

angle of 30 degrees for plates significantly larger than the members cross-section. The collapse due to instability of gusset plates is limited by the presence of transverse stiffeners welded to the web of tie plates. Moreover, whenever allowed by thickness of elements, members are connected to the gusset plate through fully welded channels. For further detail on the adopted capacity design criteria refer to standards [24–26], also recalled in design phases reported in Fig. 4.

4.3. Results of the parametric design of components

Analysing two different case studies, namely roof slabs (q_k = 1kNm^{-2}) and floors subjected to overcrowding (q_k = 3kNm^{-2}), for the bottom chord member it is evaluated the demand in terms of axial force (see Fig. 5) for different beam lengths ($L \in [L_{min} \div L_{max}]$) and spacing ($i_T \in$ [2 m÷4 m]), In fact, BB.CC. beams are designed to cover spans from 6 to 15 m (H = 600 mm), from 15 to 25 m (H = 900 mm) and from 25 to 35 m (H = 1200 mm). Fig. 6 illustrates the variation of cross-section areas required for the bottom chord member, as a function of beam-length$L$, given the yield stress $f_{(y,k)}$ of the S355J2W weathering steel, which is not constant and, according to the EN 10025–4 product standard code [30], depends on the thickness of the selected profile, taking values in the range spanning from 295 to 355 MPa.

The predominant tensile regime allows using round (R), square (SQ) or square hollow sections (SHS) profiles for the bottom chord of short, medium and high BB.CC beams, respectively. The basic profiles used for the top chord of the three BB.CC. beam families are RHS200 × 100 × t (t = 4÷12.5 mm) for H = 600 mm, RHS300 × 150 × t (t = 6÷16 mm) for H = 900 mm and RHS400 × 200 × t (t = 8÷16 mm) for H = 1200 mm. The area reduction, namely A_0-A_n, depends solely on the hole geometry and it is variable from 37% to 40% of the initial cross-section (see Fig. 2).

As already stated, chosen the basic profile, the top chord design relies on the choice of the thickness providing a suitable over-strength with respect to the bottom chord and on the evaluation of the optimal length a of tie plates, by checking the normalized slenderness $\overline{\lambda}_{f,z}$ of the compressed member with reference to its net cross-sectional area to prevent the beam lateral instability. As shown in Fig. 7, the thickness of RHS profiles has not a decisive role in the normalized slenderness of the flange under compression, even in the most demanding condition, i.e. $L = L_{max}$.

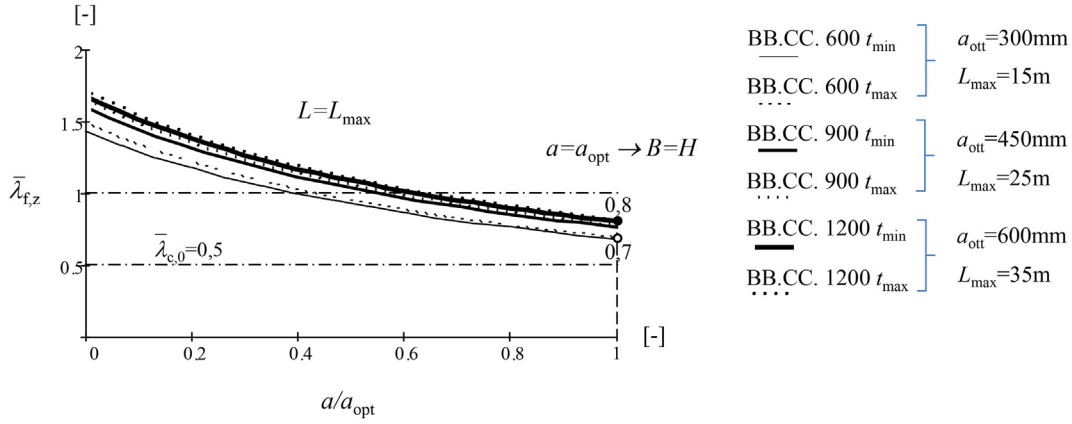

Fig. 7. Compressed flange normalized slenderness about z-axis vs. batten plate length compared to its optimal value for the three product families calculated in the worst case scenario ($L = L_{max}$).

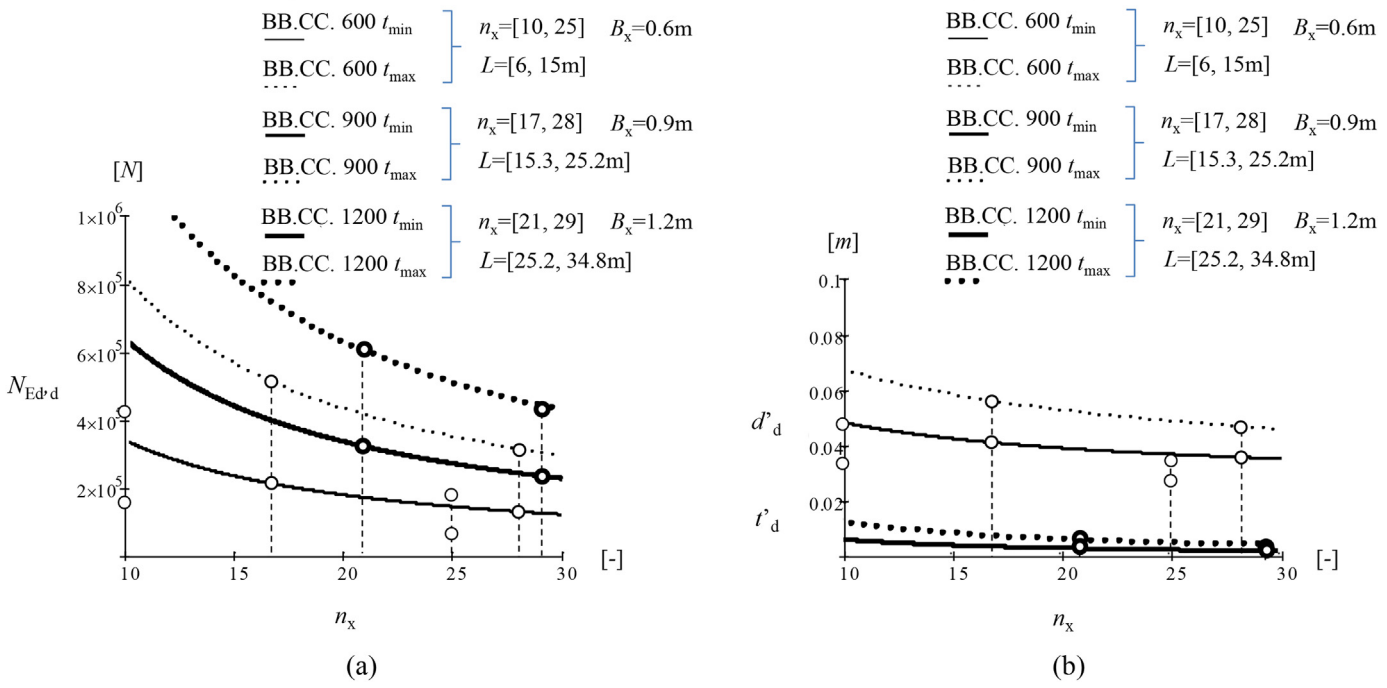

Fig. 8. Design of web diagonal members under compression as a function of the beam modules number n_x: ultimate axial load (a) and theoretical lowest diameter (b).

Introducing $r_{BH} = B/H < 2/\sqrt{3}$ as the cross-sectional shape ratio, the optimal value a_{opt} should be taken so that the beam cross-section is close to the equilateral triangle shape, allowing for the slenderness $\overline{\lambda}_{f,z}$ to remain in the range between 0.5 and 1, which appears suitable from the design viewpoint (see Fig.8). With this assumptions, it is gotten a_{opt}= 300, 450 and 600 mm for short, medium and high beams, respectively. The design process ends with definition of parameters of holes on the top chord (see Table 1 and Fig. 2).

We recall that the web members are selected to resist a design load $F_{pl,Rd}$ producing the yielding of the bottom chord at the middle-span of the beam, being $N_{Ed,\,d}$ the corresponding largest compressive force, as evaluated from Eq. (3), also displaying the relationship between the axial demand and the beam geometry. Fig. 8a shows the variation of $N_{Ed,\,d}$ as a function of the number of modules n_x. The design of these members (Fig. 8b) is done by considering the case of global shear collapse, which is a severe condition that may occur, for each product type, when the shortest space grid beam ($L = L_{min}$) is considered.

Depending on the thickness t of the C-RHS top chord profile, the web member cross-sections are R profiles with diameters in the range [30÷38 mm] or [40÷55 mm] for short beams or medium ones, respectively. In case of high beams, CHS profiles with diameter of 114.3 mm and wall thickness from 3 to 8 mm are the best choice.

The results of the design process are finally collected in Table 2, where all BB.CC. beams are identified through their own acronym and indications about profiles used for top and bottom chords and web diagonal members are given. In the same table, for the sake of completeness, the weights per unit length of beams, which are indeed useful to evaluate dead loads, costs and environmental impacts, are also indicated. Finally, aiming at ensuring BB.CC. beams with ductile behaviour, the end supports are checked towards both shear local failure and. Also in this case, the stress demand is evaluated assuming the beam collapse due to yielding of the bottom chord under the maximum global shear $V_{Ed,glob} = F_{pl,Rd}L/2$.

It is found that the most severe condition is achieved when $L = L_{min}$ and the local failure can be avoided by inserting transverse stiffeners with thickness from 5 to 10 mm, still consistent with the logic of the system prefabrication. In addition, the production cost of both web diagonal members and stiffeners of the support devices are of minor relevance on the overall production cost.

5. The beam efficiency evaluation

The BB.CC. beams can be compared to their natural competitors, namely hot-rolled laminates or welded I profiles, in terms of efficiency. The comparison is made through a suitable fast approach [31,32], proposed to compare performances of different hot-rolled profiles produced in the same country (e.g. IPE vs. HE) or even in different countries (e.g. IPE vs. UB). The adopted comparison indicator is the so-called "efficiency ratio" ρ_S, defined as:

$$\rho_S = \frac{S}{S_{SQ}} \tag{6}$$

Table 1
Opening geometric parameters for beams with $B_x = B{=}H$ (Phase 5).

Top chord				Opening parameters					
Beam type	Basic profile	Reference beam	Depth h [mm]	Initial hexagonal opening height h'_0 [mm]	Hexagon side l_h [mm]	Opening width b_h [mm]	Batten plate length a_{opt} [mm]	Final opening height (octagonal) h' [mm]	Distance between two openings w [mm]
Short 600 × t	RHS 200 × 100	IPE 200	200	200	115	231	300	500	69
Medium 900 × t	RHS 300 × 150	IPE 300	300	300	173	346	450	750	104
High 1200 × t	RHS 400 × 200	IPE 400	400	400	231	462	600	1000	138

Table 2
Abacus of BB.CC. beams resulted from the design process.

Designation			Basic profiles		
			Top chord Cold formed hollow profiles	Bottom chord Hot rolled steel bars or Square Hollow Section	Diagonal member Hot rolled steel bars or Circular Hollow Section
Beam family	Acronym	Weight per unit length G_k [kN/m]	UNI EN 10219	UNI EN 10060 UNI EN 10059 UNI EN 10219	UNI EN 10060 UNI EN 10219
Short	BB.CC._600x4	0,59	RHS 200x100x4	R38	R 30
	BB.CC._600x5	0,65	RHS 200x100x5	R42	R 30
	BB.CC._600x6	0,75	RHS 200x100x6	R46	R 32
	BB.CC._600x6.3	0,76	RHS 200x100x6.3	R47	R 32
	BB.CC._600x8	0,93	RHS 200x100x8	R52	R 36
	BB.CC._600x10	1,04	RHS 200x100x10	R58	R 36
	BB.CC._600x12,5	1,19	RHS 200x100x12.5	R63	R 38
Medium	BB.CC._900x6	1,09	RHS 300x150x6	SQ50	R 40
	BB.CC._900x6,3	1,15	RHS 300x150x6,3	SQ55	R 40
	BB.CC._900x8	1,39	RHS 300x150x8	SQ60	R 44
	BB.CC._900x10	1,66	RHS 300x150x10	SQ65	R 48
	BB.CC._900x12	1,87	RHS 300x150x12	SQ70	R 50
	BB.CC._900x12,5	1,95	RHS 300x150x12,5	SQ75	R 50
	BB.CC._900x16	2,34	RHS 300x150x16	SQ80	R 55
High	BB.CC._1200x8	1,46	RHS 400x200x8	SHS 200 × 6	CHS 114,3 × 3
	BB.CC._1200x10	1,86	RHS 400x200x10	SHS 200 × 8	CHS 114,3 × 4
	BB.CC._1200x12	2,33	RHS 400x200x12	SHS 200 × 10	CHS 114,3 × 6
	BB.CC._1200x12,5	2,37	RHS 400x200x12,5	SHS 200 × 10	CHS 114,3 × 6
	BB.CC._1200x16	2,94	RHS 400x200x16	SHS 200 × 12	CHS 114,3 × 8

being S and S_{SQ} homologous properties of the section under consideration and the benchmark one, respectively. In particular, the benchmark section is either a billet or a square profile, i.e. semi-manufactured products, having the same cross-sectional area, and thus the same weight and material unit cost, of the cross-section to be evaluated. The efficiency ratio, designed for hot-rolled profiles, is also applicable to lattice structures, if properly tailored equivalent properties S_{eq} are introduced. A similar approach is, for instance, considered in §6.4 of the EN 1993-1-1 standard [24], for analysing stability of compound grid members by assuming that bending deformability of chords must be added to the lattice shear deformability.

In the case under study, the following main geometric properties are considered for efficiency evaluation:

1) the second moment of area I_y along the strong y-axis, directly related to the bending moment performance at the Serviceability Limit State (SLS) in terms of deflection and drift;
2) the elastic section modulus $W_{el,\,y}$ and the effective shear area $A_{v,\,z}$ (actually very close to the web net area A_w) respectively connected to the bending moment and the shear strength at the Ultimate Limit State (ULS);

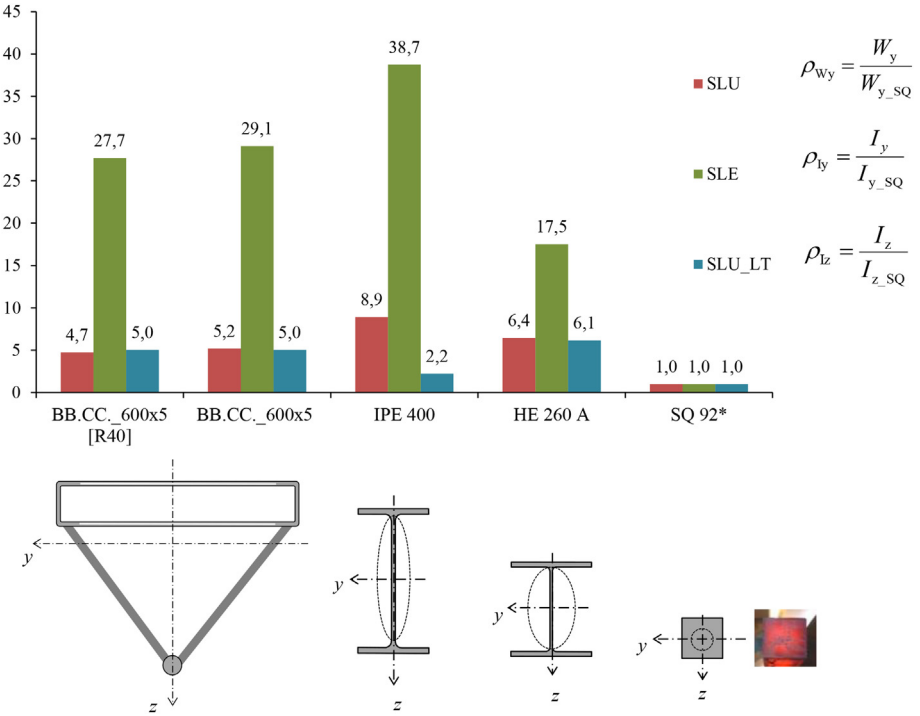

Fig. 9. Comparison among the BB. CC. 600 × 5 beam and the commonly used hot-rolled profiles with the same weight.

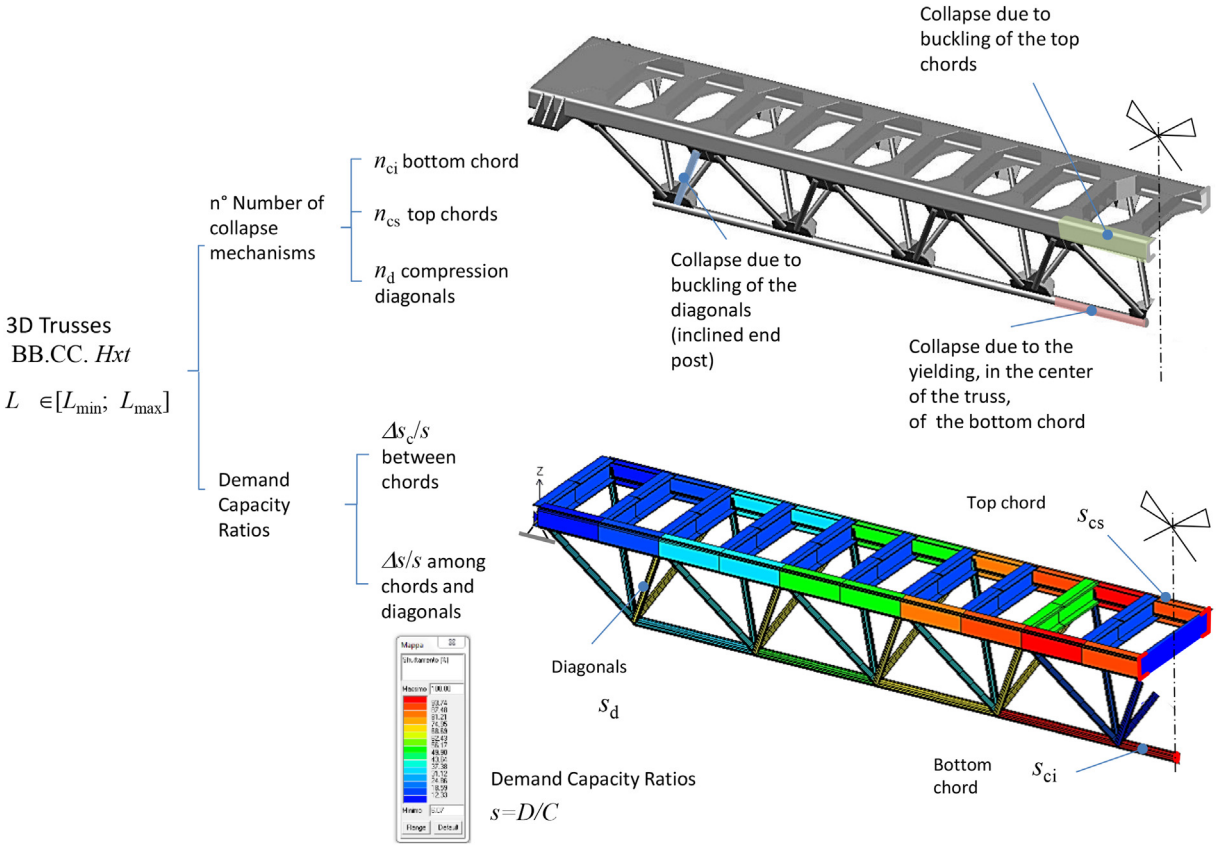

Fig. 10. An example of the FE model used to evaluate the reliability of results of the simplified design procedure.

3) the second moment of area I_z along the weak z-axis, for stability assessment at the ULS in the case of either compression or combined compressive and bending stresses;
4) the torsional constant I_t and the warping constant I_w, for evaluating the behaviour at both SLS and ULS when primary or non-uniform torsion is applied.

It is worth noticing that, from a practical design point of view, structural efficiency parameters, if properly computed for members having same cross-sectional area A (or weight G_k), allow for easily identifying the better profile in terms of performance and class of use.

As an example, let us consider the lattice beam marked as BB. CC. 600 × 5. The efficiency ratios depicted in Fig. 9 show that such a kind of beam represents a brand-new product, whose lateral-torsional bearing capacity and stiffness are respectively equal to those of wide-flange and narrow-flange profiles having the same weight.

Finally, it should be observed that, for ULS checks, medium and high BB.CC. beam families have better performances than those of HE profiles. Indeed, the lattice beams under investigation have not limitation on the flange width, which is instead limited to 300 mm for common wide-flange profiles having height equal or >300 mm.

6. A first numerical validation of the procedure

The simplified methodology for design of BB.CC. beams proposed in the present contribution has been validated through numerical analysis

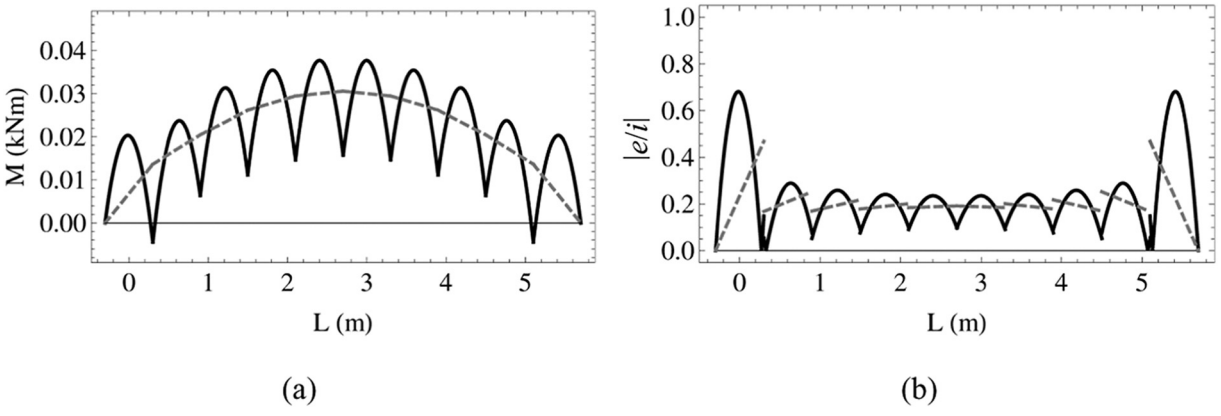

Fig. 11. Superimposition of bending moments (a) and absolute value of eccentricity over gyration radius ratios (b) along the top chord of a 6 m long BB. CC. 600 × 4 beam under symmetric transverse (1 kN/m, total), uniformly distributed (black solid thick line) and point-wise (grey dashed thick line) loads. Positive values imply that the part of the cross-section located below the neutral axis undergoes tensile stress (a). Notice that, being $|e/i| < 1$ all over the beam ($|e/i|$ is about 0.2 or less everywhere but for members close to the boundary, where at most about 0.7 is achieved), it undergoes a stretch dominated regime (b).

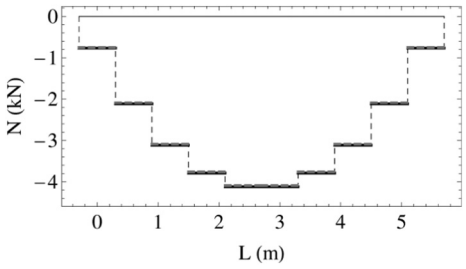

Fig. 12. Superimposition of axial forces along top chord members of a 6 m long BB. CC._600 x 4 beam under symmetric transverse (1 kN/m, total), uniformly distributed (black solid thick line) and point-wise (grey dashed thick line) loads. Negative values correspond to compression forces.

by using the FEM commercial code Pro_Sap [33] (see Fig. 10) and a home-made code (see Fig. 11) based on the principle of minimum potential energy [34], implemented in the general purpose computer algebra system Mathematica® [35]. The two codes have been used in parallel, for the sake of double blind check, for computing member forces through linear static analysis. Furthermore, the commercial code has been employed to perform modal and member check analyses, the latter according to the capacity design rules reported in the EN 1993-1-1 standard [24], also adopted by the Italian code.

The home-made code has been tailored to perform massive parametric analysis, using as main parameters the number and the geometric properties of the lattice moduli, as well as the loads distribution (i.e. symmetric or not, uniform or point-wise).

Through a large numerical campaign, by varying the span of each BB. CC. beam in a suitable range of lengths, i.e. $L_{min} \le L \le L_{max}$, the collapse mechanism under vertical loads at the ULS and a standard deviation of internal forces ratios (top to bottom chords, top chord to web member, bottom chord to web member) have been monitored. Structural performances of BB.CC. beams have been evaluated for the three beam families, analysing a sample set suitably chosen for each group of members. The set is composed of 63 FEM models for short ($H = 600$ mm)

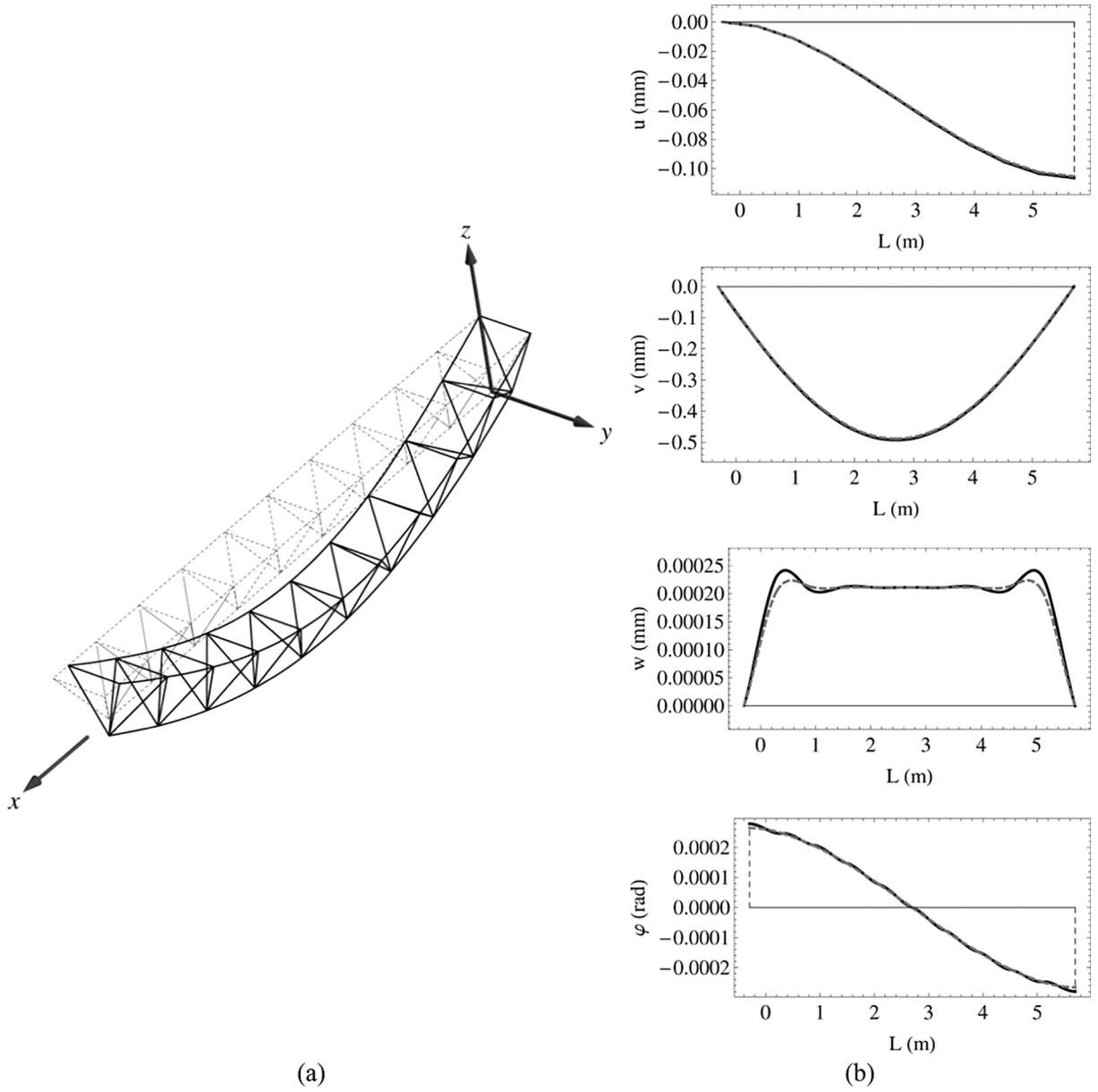

Fig. 13. Deformed shape (amplification factor of displacements: 2000) of a 6 m long BB. CC. 600 × 4 beam under symmetric distributed transverse load (1 kN/m, total) acting on top chord members (a). Superimposition of displacement and rotation functions of left top-chord line in case of distributed (black solid line) and point (grey dashed line) loads (b): from top to bottom, axial displacement u along global direction x, transverse displacements v and w along global directions z and y, rotations about y direction.

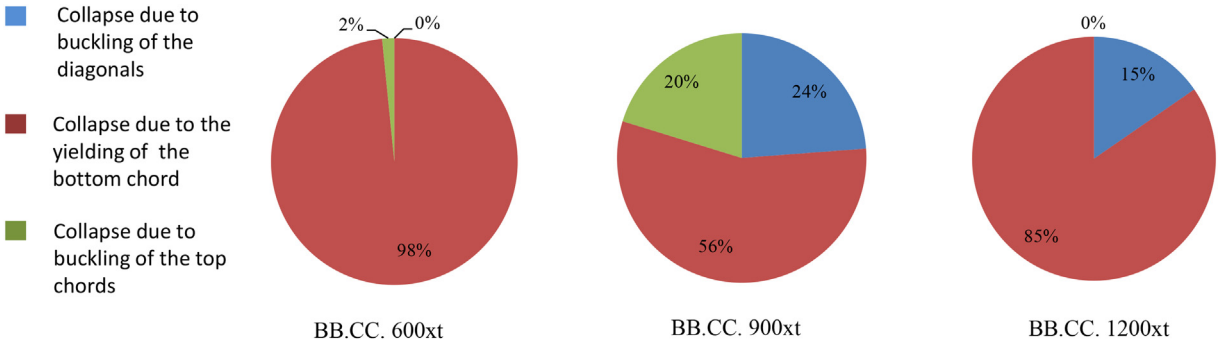

Fig. 14. Distribution of collapse mechanisms obtained from FE and parametric analyses.

beams with lengths from 6 m to 15 m, 84 FEM models for medium (H = 900 mm) beams with lengths from 6 m to 25 m and 65 FEM models for high (H = 1200 mm) beams with lengths from 6 m to 35 m (see Fig. 10). Results of both FEM computations and parametric analysis (Figs. 11–13), which are indeed very similar, showed that the investigated lattice beams undergo a stretch dominated regime (under loads, symmetric with respect to the z-axis, acting along top-chord, whatever uniformly distributed on members or concentrated on nodes), as shown in Fig. 11b where eccentricity (e) is compared to cross-sectional gyration radii (i) of members, the former being the ratio between bending moments (Fig. 11a) and axial forces (Fig. 12). This confirms that the simplest model, relying on Eqs. (1)–(5), can be suitably exploited.

The analysis of results (see Fig. 14) shows that the design criterion is particularly robust for BB.CC. beams belonging to the short and high categories. Indeed, most beams of the short family are able to develop ductile collapse (through yielding of bottom chord), without shear failure and with a 2% of analysed sample exhibiting top chord buckling.

For high beam series, the activation of brittle mechanisms involved a set of 15% of the analysed cases, which are related to beams with global shape ratios ($r_{HL} = H/L$) >1/10, currently without excessive relevance in practical applications. A worst situation is, instead, recorded for medium beams, with global shear failure affecting 24% of specimens. The high percentage of this collapse typology comes from the use of hot-rolled laminate round profiles for web members, which cannot exhibit optimal structural performances. Nevertheless, they show certain technological advantages, namely the low interference between web rods and bottom chord nodes, that make easier the manufacturing process, and good aesthetic features, with a low visual impact, which is highly relevant for applications in archaeological sites. The analysis of the scatters among exploitation indices shows in all cases an optimal utilization of chords with slight over-strength (from 5% to 15%) of the top chord with respect to the bottom one, validating the effectiveness of the over-strength coefficient Ω used in Eq. (2).

7. A brief overview on further research activities

As already stated, the presented research activity is aimed at developing a new kind of steel prefabricated beams. Therefore, in order to accomplish patenting and industrial development phases, a careful process of validation must be performed. The already performed computations are based either on simplified models or on FE model based

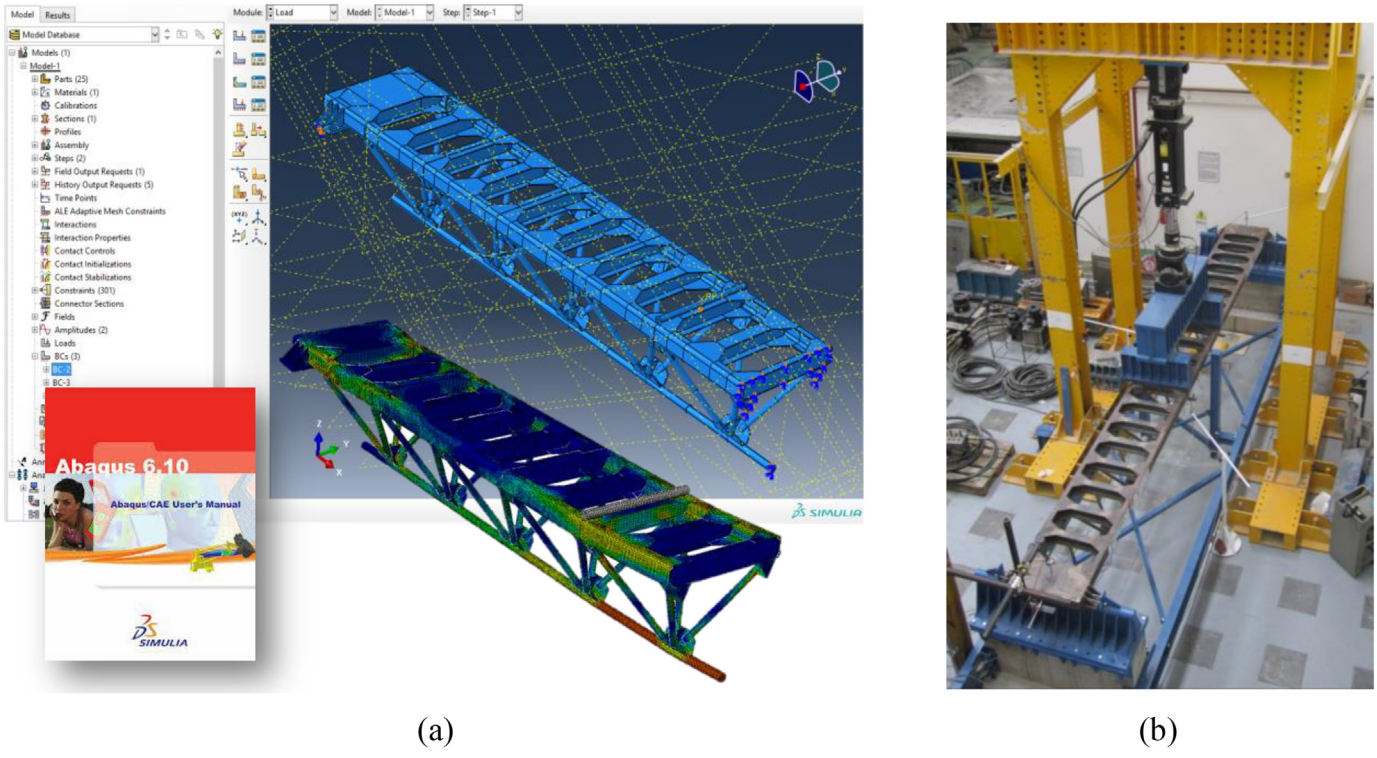

Fig. 15. Advanced investigation tools: analysis with geometric and material non-linearities (a) and full-scale test on a beam prototype (b).

on the assemblage of beam elements. More advanced computations have been already performed or are currently in progress by using two-dimensional FE model through the commercial software ABAQUS (see Fig. 15a) able to take into account geometric and material nonlinearities. Such a deeper numerical investigation is also accompanied by the experimental investigation on both S355J2W steel specimens and on BB.CC. beam full-scale prototypes up to the structural collapse (see Fig. 15b). The presentation of these numerical and experimental activities is beyond the scope of this paper and will find place in future scientific contributions.

8. Conclusions

In the current paper a simplified methodology for the design of a new steel 3D lattice beam is presented. The lattice beam is made of S355J2W weathering steel with enhanced resistance to atmospheric corrosion, which is mainly intended for protecting, in combination with structural glass panels, monumental and archaeological sites.

To this purpose, since the covering of large spans without intermediate supports is required, the use of 3D lattice beams is justified. The investigated lattice trusses have many advantages, namely high integration with the context, flexibility of use, ease of assembling and disassembling and low maintenance. Furthermore, 3D lattice trusses, after disassembly, may be conveniently reused in other environments.

The high exposure of cultural assets, which often are placed in medium-high seismicity areas, together with the use of structural glass as a roofing material, have required the definition of an adequate design methodology, based on the capacity control criteria, aimed at avoiding the occurrence of brittle collapse mechanisms. The proposed methodology, whose validity is quite general, has allowed to define three different product families of the new BB.CC. lattice beam.

The preliminary phase of the beam design has been followed by numerical investigation with different methods, for the sake of a double blind check and in order to exploit specific abilities of used methods. Results from the large campaign of numerical analysis performed have shown that the proposed design criterion is robust and able to control the collapse mechanism of each prototype in a very wide range of use, compatible with the current application fields.

Acknowledgements

The Authors gratefully acknowledge the financial support of the POR FESR 2007-2013 program for research projects developed by small and medium enterprises and research institutes. Also the contribution of the research project leader, the Sideredil s.a.s. company, is appreciatively recognized.

References

[1] United Nations Educational, Scientific and Cultural Organisation (UNESCO), Convention concerning the protection of the world cultural and natural heritage, Seventeenth Session of the General Conference, Paris, France, 16 November 1972.
[2] Legislative Decree n. 42 of 2004 January 22th, Code of the Cultural and Landscape Heritage, (in Italian), Rome, Italy 2004.
[3] E. Rosina, A. Zanelli, P. Beccarelli, M. Gargano, E. Romoli, New procedures and materials for improving protection of archaeological areas, Mater. Eval. 69 (8) (2011) 979–989.
[4] S. Ranellucci, "Archaeological Coverings. Protective installations on Archaeological Sites" (in Italian), Dei, Italy, 2009.
[5] R. Fonti, On the reading of the structural behavior of old masonry: The issue of the seismic assessment of archaeological ruins, in: T. Simos (Ed.), International Conference of Computational Methods in Sciences and Engineering (ICCMSE 2016), AIP Conference Proceedings, vol. 1790, 2016 https://doi.org/10.1063/1.4968729 , p. 130011–1130011-4, ISSN: 1551–7616, Athens, Greece, 17–20 March 2016.
[6] Z. Aslan, Protective structures for the conservation and preservation of archaeological sites, J. Conserv. Museum Stud. 3 (1997) 16–20.
[7] J. Chilton, Space Grid Structures, Architectural Press, Oxford, United Kingdom, 1999.
[8] D. Schodek, M. Bechthold, Structures, 7h ed. Pearson Education, Harlow, United Kingdom, 2014.
[9] J. Wurm, Glass Structures: Design and Construction of Self-Supporting Skins, Birkhäuser Verlag, Berlin, Germany, 2007.
[10] S. Dimova, A. Pinto, M. Feldmann, S. Denton, Guidance for European Structural Design of Glass Components: Support to the Implementation, Harmonization and Further Development of the Eurocodes, Scientific and Policy Report by the Joint Research Wurm J. Glass Structures: Design and Construction of Self-Supporting Skins, Birkhäuser Verlag, Berlin, Germany, 2007.
[11] A. Föppl, in: B.G. Teubner (Ed.), Das Fachwerk Im Raum, 1892 , Leipzig, Germany.
[12] Makowski Z. S., "Steel Space Structures" (1st ed. in English), Verlag Stahleisen GmbH, Düsseldorf, Germany, 1964.
[13] R. Landolfo, G. Di Lorenzo, O. Iuorio, M.T. Terracciano, Performance and structural potentialities of the MPN brick: the steel brick between past and future, in Italian Proc. of the XIII C.T.A. Conference, Italian Days on Steel Constructions, Ischia, Italy, 9–12 October, 2011.
[14] A. Formisano, G. De Matteis, F.M. Mazzolani, Experimental and numerical researches on aluminium alloy systems for structural applications in civil engineering fields, Key Eng. Mater. 710 (2016) 256–261, https://doi.org/10.4028/www.scientific.net/KEM.710.256.
[15] A. Formisano, F.M. Mazzolani, Numerical investigation of a new aluminium alloy reticular space structure, Civil-Comp Proceedings, 88, 9th International Conference on Computational Structures Technology (CST 2008), Athens, Greece, 2–5 September 2008, ISBN: 978-190508823-2, 2008.
[16] J. Wardenier, Y. Kurobane, J.A. Packer, G.J. van der Vegte, X.L. Zhao, Design guide for circular hollow steel sections (CHS) joints under predominantly static loading, CIDECT Design Guide, 1-2nd ed.LSS Verlag, Dortmund, Germany, 2010.
[17] F.Y. Çetin, B. İpekoğlu, Impact of transparency in the design of protective structures for conservation of archaeological remains, J. Cult. Herit. 14 (3) (2013) Supplement, Pages e21–e24.
[18] EN 10219-1:2006, Cold Formed Welded Structural Hollow Sections of Non-Alloy and Fine Grain Steels - Part 1: Technical Delivery Conditions, European Committee for Standardization, Bruxelles, Belgium, 2006.
[19] EN 10219-2:2006, Cold Formed Welded Structural Hollow Sections of Non-Alloy and Fine Grain Steels - Part 2: Tolerances, Dimensions and Sectional Properties, European Committee for Standardization, Bruxelles, Belgium, 2006.
[20] EN 1090-2:2008/A1:2011, Execution of Steel Structures and Aluminium Structures - Part 2: Technical Requirements for Steel Structures, European Committee for Standardization, Bruxelles, 2011.
[21] ISO 1006, 1983, "Building Construction – Modular Coordination – Basic Module", International Organization for Standardization, Geneva, Switzerland, 1983.
[22] J.W. Schwedeler, Theorie der Brückenbalkensysteme, Zeitschrift für Bauwesen, Berlin, 1851.
[23] R. David, Simplified assessment methods for LTB, New Steel Constr. NSC 20 (6) (2012) 24–26.
[24] EN 1993-1-1:2005/A1:2014, Eurocode 3 – Design of Steel Structures - Part 1–1: General Rules and Rules for Buildings, European Committee for Standardization, Bruxelles, Belgium, 2014.
[25] EN 1993-1-3:2006, Eurocode 3 – Design of Steel Structures - Part 1-3: General Rules - Supplementary Rules for Cold-Formed Members and Sheeting, European Committee for Standardization, Bruxelles, Belgium, 2006.
[26] EN 1993-1-5:2006, Eurocode 3 – Design of Steel Structures - Part 1–5: General Rules - Plated Structural Elements, European Committee for Standardization, Bruxelles, Belgium, 2006.
[27] M. Gündel, B. Hoffmeister, M. Fedelmann, Influence of material strength scattering on the ductile response of steel structures, Proceeding of the 11th International Conference on Applications of Statistics and Probability in Civil Engineering August 2011, pp. 465–467 , Zurich, Switzerland, 1–4.
[28] R.E. Whitmore, Experimental Investigation of Stresses in Gusset Plates, Bulletin No. 16 Engineering Experiment Station, University of Tennessee, 1952.
[29] G. Martinez-Saucedo, J.A. Packer, C. Christopoulos, Gusset plate connections to circular hollow section braces under inelastic cyclic loading, J. Struct. Eng. 134 (7) (2008) 1252–1258.
[30] EN 10025-5:2004, Hot Rolled Products of Structural steels - Part 5: Technical Delivery Conditions for Structural Steels with Improved Atmospheric Corrosion Resistance, European Committee for Standardization, Bruxelles, Belgium, 2004.
[31] G. Di Lorenzo, A. Formisano, R. Landolfo, On the origin of I beams and quick analysis on the structural efficiency of hot-rolled steel members, Open Civ. Eng. J. 11 (Suppl-1, M3) (2017) 56–70, https://doi.org/10.2174/1874149501711010332.
[32] G. Di Lorenzo, A. Formisano, R. Landolfo, Structural efficiency assessment of hot-rolled steel profiles, Proc. Int. Colloquium Stabil. Ductil. Steel Structures SDSS'2016 14 (2016) 469–476 Timisoara 30 May – 01 June 2016, ISBN: 978-929147133-1.
[33] 2S.I. Software e Servizi per l'Ingegneria S.r.l., "PRO_SAP, Version 18.1.4", https://www.2si.it/en. Date accessed: Dec. 7th, Ferrara, Italy, 2018.
[34] F. Guarracino, A. Walker, Energy Methods in Structural Mechanics: A Comprehensive Introduction to Matrix and Finite Element Methods of Analysis, Thomas Telford, United Kingdom, 1999.
[35] Wolfram Research, Inc, Mathematica, Version 8.0, Champaign, Illinois, USA, 2010.